SPHERIC 2022
INTERNATIONAL WORKSHOP

INGV
OSSERVATORIO ETNEO
SEZIONE DI CATANIA

Università di Catania

E·R·C·O·F·T·A·C

SPHERIC

SPHERIC 2022

CATANIA, ITALY, 6–9 JUNE 2022

Proceedings of the 16th SPHERIC International Workshop

Edited by
Giuseppe Bilotta

SPHERIC 2022

Proceedings of the 16th SPHERIC International Workshop

Catania, Italy, 6–9 June 2022
Istituto Nazionale di Geofisica e Vulcanologia
Università di Catania

Edited by
Giuseppe Bilotta

Published by the Istituto Nazionale di Geofisica e Vulcanologia
ISBN 979-12-8028-205-7

Acknowledgements

The 16th SPHERIC International Workshop is supported by the Osservatorio Etneo of the Istituto Nazionale di Geofisica e Vulcanologia, the Università di Catania and ERCOFTAC.

INGV OSSERVATORIO ETNEO SEZIONE DI CATANIA

Università di Catania

ERCOFTAC

To our colleagues from the Osservatorio Etneo, Monastero dei Benedettini, Museo della Rappresentazione and the Laboratorio di Idraulica go our deepest and sincere thanks for their logistical support. Our gratitude extends to all the members of the SPHERIC Steering Committee, and the chair and vice chair in particular, for their continued guidance in the organization of the workshop. This Workshop would not have been possible without your support.

SPHERIC 2022
INTERNATIONAL WORKSHOP

Cover photo: May 2022 Mt Etna eruption © Francesco Zuccarello.

Foreword

Dear Delegate,

the Osservatorio Etneo, Catania section of the Istituto Nazionale di Geofisica e Vulcanologia, in collaboration with the Università di Catania, is delighted to host the 16th SPHERIC International Workshop.

SPHERIC, the ERCOFTAC Special Interest Group that represents the community of researchers and industrial users of Smoothed Particle Hydrodynamics, has made outstanding efforts to support and foster the development of SPH with online and hybrid events in these difficult times, finding new and creative ways to bring people together and keep the interest for SPH alive inside and outside the community. The choice between a virtual and an on-site event for the 16th edition of the SPHERIC International Workshops has been a difficult one to make. On the one hand, the still problematic international situation would have obstructed participation; on the other, the kind and level of inter-personal exchange that can only be achieved by meeting in-person remains an important aspect of the scientific growth of the community. We have taken a gamble of sorts, and we appreciate the effort of all of you, those that have had the opportunity to come, as well as those that could not make it, in supporting our choice.

In the now well-established tradition of the SPHERIC International Workshops, the programme of this edition offers a Training Day for researchers and users that are starting their work on SPH, and two challenging keynotes. As usual, the Libersky Prize will be awarded for the best contribution from student delegates; the 16th SPHERIC International Workshop also presents for the third time the Joe Monaghan Prize, a recognition to the most important work published on the SPHERIC Grand Challenges between 2013 and 2018.

The contributions that you can find in these Proceedings were selected by our Scientific Committee from over 80 high-level proposed abstracts. They are a testament to the excellent quality of the research being conducted both on the fundamentals of the SPH method and on its application to a wide variety of fields, from engineering to medicine, from geophysics to material sciences.

New and exciting times await Smoothed Particle Hydrodynamics and the SPHERIC community, and it is a great pleasure and honour to share these moments with you.

Come for the science, stay for the food!
Welcome to Catania,

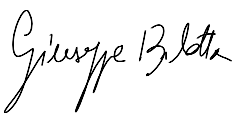

Giuseppe Bilotta
Chair, Local Organizing Committee
16th SPHERIC International Workshop

Scientific Committee

Dr. Alex Crespo (Universidade de Vigo, Ourense, Spain)
Dr. Abbas Khayyer (Kyoto University, Japan)
Dr. David Le Touzé (Ecole Centrale de Nantes, France)
Dr. Nathan Quinlan (National University of Ireland, Galway, Ireland)
Dr. Stefano Sibilla (Università di Pavia, Italy)
Dr. Angelo Tafuni (New Jersey Institute of Technology, US)
Dr. Renato Vacondio (Università di Parma, Italy)
Dr. Antonio Gil (Swansea University, UK)
Dr. Andrea Colagrossi (CNR-INM, Italy)
Dr. Ben Rogers (University of Manchester, UK)
Dr. Salvatore Marrone (CNR-INM, Italy)
Dr. Peter Eberhard (University of Stuttgart, Germany)
Dr. Matthieu De Leffe (Siemens Digital Industries, France)
Dr. Giuseppe Bilotta (Istituto Nazionale di Geofisica e Vulcanologia, Italy)
Dr. Ha Bui (Monash University, Australia)
Dr. Raj Das (RMIT University, Australia)
Dr. Steven Lind (University of Manchester, UK)
Dr. Georgios Fourtakas (University of Manchester, UK)
Dr. Chun Hean Lee (Universiy of Glasgow, UK)
Dr. Moncho Gómez-Gesteira (Universidade de Vigo, Spain)
Dr. Xu Fei (Northwestern Polytechnical University, China)
Dr. Antonio Souto Iglesias (UPM, Spain)
Dr. Rouhollah Fatehi (Persian Gulf University, Iran)
Dr. Xiangyu Hu (Technical University of Munich, Germany)
Dr. Pengnan Sun (Sun Yat-sen University, China)
Dr. Tom De Vuyst (University of Hertfordshire, UK)

Local Organizing Committee

Dr. Giuseppe Bilotta
Dr. Annalisa Cappello
Dr. Gaetana Ganci

Table of contents

Convergence, consistency and stability I (S1)

1.1 A novel LES perspective on SPH & the issue of particle duality 1
Max Okraschevski, Niklas Bürkle, Rainer Koch, Hans-Jörg Bauer

1.2 Implicit Iterative Shifting in ALE-SPH schemes 9
Pietro Rastelli, Renato Vacondio, Jean-Christophe Marongiu

1.3 An Updated Reference Lagrangian SPH algorithm for isothermal elasticity and thermo-elasticity . 17
Chun Hean Lee, Paulo R. Refachinho de Campos, Antonio J. Gil, Javier Bonet

1.4 An hourglass control implementation for total Lagrangian SPH 25
Dong Wu, Chi Zhang, Xiaojing Tang, Xiangyu Hu

Boundary Conditions (S2)

2.1 Droplet-pressure wave interactions using a Young-Laplace pressure based boundary condition . . 33
Michael Blank, Sandeep Shah, Prapanch Nair, Thorsten Poeschel

2.2 A Lagrangian free-stream boundary condition for weakly compressible smoothed particle hydrodynamics 40
Shuoguo Zhang, Wenbin Zhang, Xiangyu Hu

2.3 Transverse Velocity Discontinuities at Material Interfaces in the Compressible Euler Equations with SPH 47
Jason M. Pearl, Cody D. Raskin, J. Michael Owen

2.4 Development of a modelling strategy for cyclic asymmetric problems using the SPH approach . . 55
Daniel M. Aguirre Bermudez, Max Okraschevski, Niklas Bürkle, Corina Schwitzke, Hans-Jörg Bauer

Solids and structures (S3)

3.1 SPH modelling of fragmentation of brittle planar and spherical targets 63
Tom De Vuyst, Rade Vignjevic, Mikhail Glazunov

3.2 A coupled total Lagrangian SPH-phase-field framework for modeling dynamic brittle fracture . . 71
Mohammad Naqib Rahimi, Georgios Moutsanidis

3.3 Innovative Fragmentation Modelling of Hypervelocity Impacts 77
Anthony Collé, Jérôme Limido, Thomas Unfer

3.4 Numerical study of solid particle erosion using smoothed particle hydrodynamics 84
Shoya Mohseni-Mofidi, Claas Bierwisch, Eric Drescher, Harald Kruggel-Emden

Alternative and novel formulations (S4)

4.1 DEM-WCSPH Modeling of Hydroelastic Slamming 91
Salvatore Capasso, Bonaventura Tagliafierro, Alejandro J.C. Crespo, Iván Martínez-Estévez, José M. Domínguez, Moncho Gómez-Gesteira, Giacomo Viccione

4.2 Boundary integral approach for axisymmetric SPH 99
Martin Ferrand, Zixing Dong, Damien Violeau

4.3 Smoothed Particle Hydrodynamics Realisation of Finite Volume Method for Fluid-Structure Interaction 107
Zhentong Wang, Oskar J. Haidn, Chi Zhang, Xiangyu Hu

4.4 Axisymmetric magneto-hydrodynamics with SPH 115
Domingo García-Senz, Robert Wissing, Rubén M. Cabezón

Practical and industrial applications I: automotive and aerospace engineering (S5)

5.1 Industry-relevant validation cases for benchmarking SPH cases 123
Georg A. Mensah, Leonid Braun, Shriram Krishna, Pierre Sabrowski, Tobias B. Wybranietz

5.2 Aerodynamic coupling to smoothed particle hydrodynamics for modelling aircraft fuel-jettison . . 130
James MacLeod, Thomas Rendall

5.3 Local numerical and experimental comparisons of a tire rolling over a puddle of water using a coupled SPH-FE strategy and the r-PIV technique 138
Arbia Ben Khodja, Corentin Hermange, Serge Simoëns, Marc Michard, Guillaume Oger, David Le Touzé

5.4 Snow Soiling Simulation of Automotive Vehicles using SPH 146
Fabian Meyer, Marian Majda, Shreyas Joshi

Convergence, consistency and stability II (S6)

6.1 δ-ULSPH: Updated Lagrangian SPH structure model enhanced through incorporation of δ-SPH density diffusion term 154
Abbas Khayyer, Yuma Shimizu, Chun Hean Lee, Kazuhiro Kinuta, Antonio J. Gil, Hitoshi Gotoh, Javier Bonet

6.2 An immersed boundary pseudo-spectral ISPH scheme 162
Joseph O'Connor, Georgios Fourtakas, Benedict D. Rogers

6.3 Analysis through energy consideration of a quasi-Lagrangian scheme using Riemann stabilization 170
Julien Michel, Salvatore Marrone, Matteo Antuono, Guillaume Oger

6.4 Modified Dynamic Stabilization scheme for ISPH simulations 178
Naoki Tsuruta, Abbas Khayyer, Hitoshi Gotoh

6.5 Adjusting numerical viscosity of contact SPH method at modelling realistic compressible flows . 186
Georgii D. Rublev, Anatoly N. Parshikov, Sergey A. Dyachkov, Stanislav A. Medin

Free-surface flow and moving boundaries (S7)

7.1 Weakly-compressible SPH schemes with an acoustic-damper term 192
Peng-Nan Sun, Chiara Pilloton, Matteo Antuono, Andrea Colagrossi

7.2 Energy dissipation evaluation in violent 3D sloshing flows subject to vertical accelerations . . . 200
Julien Michel, Danilo Durante, Salvatore Marrone, Andrea Colagrossi

7.3 SPH prediction of energy dissipation in a sloshing tank subjected to vertical harmonic excitations . 208
Salvatore Marrone, Francesco Saltari, Julien Michel, Franco Mastroddi

7.4 Extension and Validation of SPHinXsys, an open-source multi-physics SPH library, for simulation of sloshing flows with elastic baffles 216
Yaru Ren, Abbas Khayyer, Pengzhi Lin

Practical and industrial applications II: coastal and ocean engineering (S8)

8.1 SPH simulation of wave breaking over a barred beach 223
Pietro Scandura, Corrado Altomare, Ivan Caceres, Giacomo Viccione, Dominic van der A

8.2 Restoring and rehabilitation of historical coastal asset with SPH 229
Corrado Altomare, Xavier Gironella, Alejandro J.C. Crespo, José M. Domínguez, Angelo Tafuni, Gregori Muñoz-Ramos

8.3 Validation of an SPH-FEM model for offshore structure 237
Vito Zago, Noura Almashan, Robert A. Dalrymple, Giuseppe Bilotta, Dana B. Al-Houti, Subramaniam Neelamani

8.4 Simulation of a flexible fish farming net in currents and waves with DualSPHysics 245
Raúl González-Ávalos, Corrado Altomare, Xavier Gironella, Alejandro J.C. Crespo, Iván Martínez-Estévez

Geophysics, geotechnics and disaster simulation (S9)

9.1 SPH scheme for multifluid open flow with discontinuous nonlinear viscosity 253
Juan Gabriel Monge-Gapper, Alberto Serrano-Pacheco, Daniel Duque, Javier Calderon-Sanchez

9.2 SPH modelling of poroelasticity based on **u**-**w**-p Biot's formulation 261
Cong Yao, Georgios Fourtakas, Benedict D. Rogers, Domenico Lombardi

9.3 Modelling rainfall-induced slope collapse with Smoothed Particle Hydrodynamics 268
Ruofeng Feng, Georgios Fourtakas, Benedict D. Rogers, Domenico Lombardi

9.4 Validation of viscous flows in DualSPHysics: application to mudflow behaviours 276
Suzanne Lapillonne, Georgios Fourtakas, Guillaume Piton, Vincent Richefeu

Viscosity and turbulence (S10)

10.1 A Large Eddy Simulation SPH scheme for bubbly free-surface flows 283
Jack King, Steven J. Lind, Benedict D. Rogers, Peter K. Stansby, Renato Vacondio

10.2 The role of the viscosity model in predicting losses in systems with rotating fluids using smoothed particle hydrodynamics 289
Ubaid Ali Qadri, Stephen Longshaw, Aaron English, Benedict D. Rogers, Georgios Fourtakas

10.3 High-order SPH schemes for DNS of turbulent flow 295
Francesco Ricci, Renato Vacondio, Angelo Tafuni

10.4 Dam Break Flow Benchmarks: Quo Vadis? 301
Giordano Lipari, Andrea Colagrossi

Complex physics (S11)

11.1 SPH Simulation of Active Matters 309
Roozbeh Saghatchi, Deniz C. Kolukisa, Mehmet Yildiz

11.2 An integrative SPH for cardiac function with network 315
Chi Zhang, Xiangyu Hu, Hao Gao

11.3 SPH Model of Human Breathing with and without Face Coverings 323
Aaron English, Benedict D. Rogers, Georgios Fourtakas, Steven J. Lind, Peter K. Stansby

11.4 Lagrangian methods in SPH for complex systems 329
Antonio Souto-Iglesia, Josep Bonet Avalos, Matteo Antuono, Andrea Colagrossi

11.5 Unified simulation of multi-material flows with SPH-FVM coupling algorithm 336
Rodion V. Muratov, Sergey A. Dyachkov

Adaptivity, efficiency and acceleration (S12)

12.1 Hybridized guard particles for Adaptive Particle Refinement 344
Joffrey Chanéac, Stéphane Aubert, Pierre Duquesne, Jean-Christophe Marongiu

12.2 Localized kernel gradient correction for SPH simulations of water wave propagation 352
Lennart J. Schulze, Vito Zago, Giuseppe Bilotta, Robert A. Dalrymple

12.3 GPU-accelerated Explicit Incompressible-Compressible SPH for multi-phase flow with large density difference 360
Hee Sang Yoo, Young Beom Jo, Eung Soo Kim

SPH in software: preprocessing, post-processing and high-performance computing **(S13)**

13.1 A level-set based self-cleaning pre-processing tool for particle-based methods 368
Yongchuan Yu, Oskar J. Haidn, Yujie Zhu, Chi Zhang, Xiangyu Hu

13.2 A new isosurface reconstruction tool for SPH complex geometry preprocessing 376
Jiatao Zhang, Xiaohu Guo, Xiufang Feng, Li Zhu

13.3 Building Automatic Regression Test Environment for Open-source Scientific Library SPHinXsys . 383
Bo Zhang, Chi Zhang, Xiangyu Hu

13.4 Preparing SPH for the Exascale Computing Revolution 391
Benedict D. Rogers, Richard Bower, Matthieu Schaller, Abouzied Nasar, Georgios Fourtakas, Scott Kay, Alasdair Basden, Tobias Weinzierl, Peter Draper, Stephen Longshaw, Tom De Vuyst

Practical and industrial applications III: thin film mechanics **(S14)**

14.1 Numerical simulation of ultra-thin-flexible structures in SPH: an embedded FEA structural solver within DualSPHysics 399
Joe El Rahi, Ivan Martínez-Estévez, Bonaventura Tagliafierro, José M. Domínguez, Alejandro J.C. Crespo, Vasiliki Stratigaki, Tomohiro Suzuki, Moncho Gómez-Gesteira, Peter Troch

14.2 Thin Film Flow Dynamics in Gas-Liquid Contact Reactors 406
Cihan Ates, Karthik Vigneshwaran Muthukumar, Max Okraschevski, Niklas Bürkle, Daniel M. Aguirre Bermudez, Matthias Haber, Rainer Koch, Hans-Jörg Bauer

14.3 Detecting Laminar Mixing Patterns in Twin-screw Extruder Elements via Lagrangian Coherent Structures 414
Hannes Bauer, Johannes Khinast

Lagrangian methods in SPH for complex systems

Antonio Souto-Iglesias
CEHINAV, DACSON, ETSIN,
Universidad Politécnica de Madrid,
Madrid, Spain,
antonio.souto@upm.es

Josep Bonet Avalos
Dep. d'Enginyeria Química, ETSEQ,
Universitat Rovira i Virgili,
Tarragona, Spain,
josep.bonet@urv.cat

Matteo Antuono & Andrea Colagrossi
CNR-INM Institute of marine engineering
National Research Council
Rome, Italy,
matteo.antuono@cnr.it, andrea.colagrossi@cnr.it

***Abstract*—The application of Lagrangian mechanics in combination with the definition of the dissipative function concept, first introduced by Rayleigh, to the construction of Smoothed Particle Hydrodynamics (SPH) equations for complex systems and situations is reviewed in this article. To illustrate the method, we have addressed the non-trivial problem of a micropolar fluid for which we have derived the most general expression for the friction forces related to particle velocities coupled to particle spin, for translational as well as for the rotational motion of the SPH particles. For the latter we have also discussed the scaling of the moment of inertia in SPH with the range of the weight function, and also with regards to the microscopic moment of inertia. The comparison of the SPH results with known solutions of the dynamics of micropolar fluids yields an excellent agreement.**

I. Introduction

Recently, we have addressed the application of Smoothed Particle Hydrodynamics (SPH) to complex situations in a series theoretical works, which involve the analysis of the Stokes hypothesis [5], modification of SPH to include arbitrary bulk viscosity contributions [3], and the construction of the SPH equations for a general micropolar fluid [19]. The difficulties of defining the appropriate SPH equations of motion beyond the standard ones are overcome using a Lagrangian formulation of an ensemble of particles rather than the customary discretization of the field equations, notably, the Navier-Stokes equation. While there are precedents of the use of Lagrangians in SPH, [24], we have exploited the introduction of a *Dissipation Function*(DF), which gives a great flexibility for the modelling of the dissipation terms to be included in the equations of motion. In this way, Lagrangian symmetries, such as Galilean and rotational invariance that lead to total momentum and angular momentum conservation, for instance, are imposed to the DF with the result of SPH equations of motion which also conserve these properties, regardless the complex form of the dissipative forces. Some of the most remarkable outcomes are the model for bulk viscosity modelled independently of shear viscosity, which is relevant for hypersonic flow, as well as to construct the SPH equations for the most general micropolar fluid model. These two examples clearly show the importance of the use of the DF in producing SPH descriptions of complex fluids and fluxes for applications to complex micorstructured fluids and extreme flows. In this communication we will present the general principles of our approach exemplified in the isotropic micropolar fluid. We show how the continuum equations of motion of the latter [6] can be reproduced by an array of SPH particles with rotational degrees of freedom, which interact with each other through appropriate frictional forces derived from the DF, in a general way. The micropolar SPH equations have been validated by comparing our 3D simulations with analytical solutions as well as numerical results for different geometries, such as the lid-driven cavity [23], among others, with excellent agreement.

II. Equations of motion for fluids with spin

A. The SPH approximation to the hydrodynamic fields

Let us consider an ensemble of N isotropic particles representing fluid elements located at positions $\boldsymbol{r}_i$, $i = 1, \ldots, N$ with velocities $\boldsymbol{u}_i$, masses m_i, and associated volumes V_i. Since the particles are considered as macroscopic objects, representative of a large quantity of microscopic particles of the physical fluid, we can define the internal energy per unit of mass e_i along with the particle entropy per unit of mass s_i. To model micropolar fluids, we assume that the particles are isotropic but that they can rotate, thus bearing angular momentum. In SPH, fields are associated to corresponding physical properties carried by particles, or defined from the immediate neighborhood. The main example of the latter is the particle mass density:

$$\rho_i = m_i \sum_{j=1}^{N} W(r_{ij}; h), \tag{1}$$

where W is a weight function referred to as kernel. Here, $\boldsymbol{r}_{ij} = \boldsymbol{r}_i - \boldsymbol{r}_j$ and $r_{ij} = |\boldsymbol{r}_{ij}|$. The particle volume V_i is estimated as

$$V_i = \frac{m_i}{\rho_i} = \frac{1}{\sum_{j=1}^{N} W(r_{ij}; h)}. \tag{2}$$

The kernel W is a positive-definite monotonously decreasing integrable function with a characteristic length h (see [25] for a recent discussion on the choice of kernels' characteristic length), which will be omitted in the notation where no confusion could occur. In this article, this kernel is isotropic and its volume integral is normalized, i.e.

$$\int d\boldsymbol{r}\, W(r) = 1. \tag{3}$$

The spatial gradient of the kernel satisfies

$$\nabla_i W(r_{ij}) = \boldsymbol{e}_{ij}\frac{dW}{dr_{ij}} = -\boldsymbol{r}_{ij}F(r_{ij}) = -\nabla_j W(r_{ij}), \tag{4}$$

where $\boldsymbol{e}_{ij} = \boldsymbol{r}_{ij}/r_{ij}$ is a unit vector, and F is defined from this equation, being a positively definite function by construction.

In SPH, to reproduce smooth fields, insensitive to the underlying particulate nature of the description, it is required that $V_i \ll h^n$ (n is the dimensionality of the space), i.e. that the number of particles ν in a given particle environment, determined by the range of the kernel h, must be large enough. Moreover, to recover the hydrodynamic behavior, as described by the Navier-Stokes equation, the so-called hydrodynamic limit must be invoked [12]. The latter states that the characteristic wavelengths of the fields must be much larger than h so that spatial variations of the fields up to $O(k^2)$ are sufficient to describe the dynamics, k being the field wave number. Hence, if $L \sim 1/k$ is the characteristic length for the variation of a hydrodynamic field, the continuous limit description should be reached when $h/L \sim kh \to 0$ with $V_i/h^n \to 0$ [7], [14], [18].

Following the approach of [5], the conservative dynamics of the system can be derived from the Lagrangian

$$\begin{aligned}\mathcal{L}[\dot{\boldsymbol{r}}_i, \boldsymbol{r}_i, \dot{\boldsymbol{\theta}}_i, \boldsymbol{\theta}_i] \;=\; & \sum_i \left[\frac{1}{2}\left(m_i\,\dot{r}_i^2 + m_i\,I_i\,\dot{\boldsymbol{\theta}}_i^{\,2}\right) - m_i\,U(t,\boldsymbol{r}_i) - \right.\\ & \left. -\; m_i\,\mathcal{V}(t,\boldsymbol{\theta}_i) - m_i\,e(\rho_i, s_i)\right],\end{aligned} \tag{5}$$

where the first term on the right hand side of this equation is the kinetic energy of the particles, which includes a translational and a rotational term. The rotational term is computed considering an additional rotational degree of freedom, $\boldsymbol{\theta}_i$, representing the angular displacement, and the particle inertia per unit mass, I_i. In equation 5, U is a general external potential field such as gravity, $\mathcal{V}$ is an external potential field leading to a body torque. In addition, we define the velocity $\dot{\boldsymbol{r}}_i = \boldsymbol{u}_i$, and we denote $\boldsymbol{\Omega}_i = \dot{\boldsymbol{\theta}}_i$, referring to it as the *spin*, from now on. Finally, e is the *internal energy*, which is considered to be a function only on the particle thermodynamic state properties density, ρ_i, and entropy, s_i, in the present model.

To introduce the dissipative forces for rotating particles, let us first consider that the viscous dissipation is generated due to friction at the contact point of the volume occupied by the particles, defined as the mid point between the centers of the two interacting particles i, and j. The composition of the translational velocity and the velocity induced by the spin (see Fig. 1) at such contact point leads to the following velocity difference at contact

$$\boldsymbol{u}^*_{ij} = \boldsymbol{u}_{ij} - \overline{\boldsymbol{\Omega}}_{ij} \times \boldsymbol{r}_{ij}, \tag{6}$$

with $\boldsymbol{u}_{ij} = \boldsymbol{u}_i - \boldsymbol{u}_j$ and $\overline{\boldsymbol{\Omega}}_{ij} := (\boldsymbol{\Omega}_i + \boldsymbol{\Omega}_j)/2$.

The assumption that the contact point can be considered as the mid point is the result of assuming that the boundaries between two adjacent particles are placed at the mid point, and therefore there is where the friction is located. Other options could be considered but one expects they would not significantly affect the long-wavelength behavior of the system.

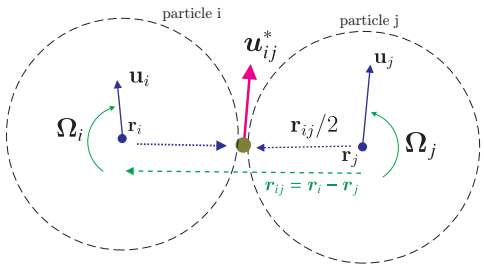

Fig. 1. Schematic representation of two interacting particles, with internal rotation, including all the variables necessary to define $\boldsymbol{u}^*_{ij}$.

Together with the Lagrangian, following [3], [5], [8] we define the dissipation function, often referred to as Rayleighian, as a positive-definite bilinear form of the velocity difference at contact,

$$\Phi_D = \sum_{i,j>i} \boldsymbol{u}^*_{ij} \cdot\; \mathbb{A}_{ij}(r_{ij}) \;\cdot \boldsymbol{u}^*_{ij}, \tag{7}$$

where the tensor $\mathbb{A}_{ij}(r_{ij})$ is given by

$$\mathbb{A}_{ij}(r_{ij}) \;=\; F(r_{ij})\,(\zeta_1\,\boldsymbol{e}_{ij} \otimes \boldsymbol{e}_{ij} + \zeta_2\,\boldsymbol{I})\,V_i V_j, \tag{8}$$

in which the coefficients ζ_1, ζ_2 have dimensions of dynamic viscosities. The right hand side of (8) is the most general second rank isotropic *objective* tensor, constructed from particle coordinates [21]. So defined, and considering the form of the $\boldsymbol{u}^*_{ij}$, this dissipation function is as general as it can be in regards to being invariant to translations and rigid rotations. These imposed symmetries in the dissipation function are analogous to the symmetries of the Lagrangian. Effectively, if the dissipation function is invariant under translations and solid body rotations, the total momentum as well as the total angular momentum of the system will be unaffected by the dissipative forces derived from the former.

In view of (7) and (8), the DF takes the form,

$$\begin{aligned}\Phi_D =& \frac{\zeta_1}{2}\sum_{i,j\neq i} F(r_{ij})\,(\boldsymbol{e}_{ij}\cdot\boldsymbol{u}_{ij})^2\,V_i V_j + \\ &+\; \frac{\zeta_2}{2}\sum_{i,j\neq i} F(r_{ij})\left(\boldsymbol{u}_{ij} - \overline{\boldsymbol{\Omega}}_{ij}\times\boldsymbol{r}_{ij}\right)^2 V_i V_j,\end{aligned} \tag{9}$$

where the summation takes now each pair twice, a convention which is possible due to the symmetry of the interactions, and that facilitates some of the deductions later on. Since $F(0) = 0$ for common kernels, the restriction $j \neq i$ in the summation in this equation, and in the ones that follow in the rest of the paper, could ultimately be removed.

The second term in (9) is the new contribution proposed, and represents the friction between two particles due to the velocity difference in the mid point between the particles, induced by the translational velocities and the spin induced ones.

Notice that in eqs. (5) and (9) we have made the distinction

between the independent variables in the Lagrangian $\dot{\boldsymbol{r}}_i, \boldsymbol{r}_i$, $\dot{\boldsymbol{\theta}}_i$, $\boldsymbol{\theta}_i$ and the ones in the Rayleighian $\boldsymbol{u}_i$, $\boldsymbol{\Omega}_i$, although one assumes that $\dot{\boldsymbol{r}}_i = \boldsymbol{u}_i$ and $\dot{\boldsymbol{\theta}}_i = \boldsymbol{\Omega}_i$, at the end. Moreover, the dissipation function must be a quadratic function of the velocities. Under these conditions, the dynamics of the system is given by

$$\begin{cases} \dfrac{d}{dt}\left(\dfrac{\partial \mathcal{L}}{\partial \dot{\boldsymbol{r}}_i}\right) - \dfrac{\partial \mathcal{L}}{\partial \boldsymbol{r}_i} = \mathcal{Q}_i^V, \\ \dfrac{d}{dt}\left(\dfrac{\partial \mathcal{L}}{\partial \dot{\boldsymbol{\theta}}_i}\right) - \dfrac{\partial \mathcal{L}}{\partial \boldsymbol{\theta}_i} = \mathcal{T}_i^V, \end{cases} \tag{10}$$

where $\mathcal{Q}_i^V$, $\mathcal{T}_i^V$ are, respectively, the generalized dissipative forces and torques acting among the particles, which are obtained from differentiation of Φ_D with respect to $\boldsymbol{u}_i$ and $\boldsymbol{\Omega}_i$, respectively, i.e.

$$\begin{aligned} \mathcal{Q}_i^V = -\frac{\partial}{\partial \boldsymbol{u}_i}\Phi_D = &-\zeta_1 \sum_j F(r_{ij}) \left(\boldsymbol{u}_{ij}\cdot\boldsymbol{e}_{ij}\right)\boldsymbol{e}_{ij} V_i V_j \\ &-\zeta_2 \sum_j F(r_{ij}) \left(\boldsymbol{u}_{ij} - \overline{\boldsymbol{\Omega}}_{ij}\times\boldsymbol{r}_{ij}\right) V_i V_j, \end{aligned} \tag{11}$$

$$\mathcal{T}_i^V = -\frac{\partial}{\partial \boldsymbol{\Omega}_i}\Phi_D = \frac{\zeta_2}{2}\sum_j F(r_{ij})\,\boldsymbol{r}_{ij}\times\left(\boldsymbol{u}_{ij} - \overline{\boldsymbol{\Omega}}_{ij}\times\boldsymbol{r}_{ij}\right) V_i V_j. \tag{12}$$

Eq (11) can be written as

$$\begin{aligned} \mathcal{Q}_i^V = -\frac{\partial}{\partial \boldsymbol{u}_i}\Phi_D = &-\zeta_1 \sum_j F(r_{ij}) \left(\boldsymbol{u}_{ij}\cdot\boldsymbol{e}_{ij}\right)\boldsymbol{e}_{ij} V_i V_j \\ &-\zeta_2 \sum_j F(r_{ij})\,\boldsymbol{u}_{ij} V_i V_j \\ &+\zeta_2 \sum_j F(r_{ij})\,(\overline{\boldsymbol{\Omega}}_{ij}\times\boldsymbol{r}_{ij})\, V_i V_j, \end{aligned} \tag{13}$$

Notice that, by construction, the dissipative forces and torques can be split into pairwise contributions, i.e. $\mathcal{Q}_i^V = \sum_{j\neq i}\mathcal{Q}_{ij}^V$ and $\mathcal{T}_i^V = \sum_{j\neq i}\mathcal{T}_{ij}^V$, with

$$\begin{aligned} \mathcal{Q}_{ij}^V &= -\mathcal{Q}_{ji}^V \\ \mathcal{T}_{ij}^V &= \mathcal{T}_{ji}^V \end{aligned} \tag{14}$$

With this notation, as discussed in [5], the first contribution in (13) corresponds to the Monaghan and Gingold's viscous term [15], and the second to the Morris et al. viscous term [16]. However, the first term conserves angular momentum while the second does not. As will be seen later in the paper, the third term, the contribution due to the spin and the related spin derivative equation, will allow to correct this matter.

The equation of motion for the roto-translational dynamics of the ensemble of particles obtained from (10) reads:

$$\begin{cases} m_i\dfrac{d\boldsymbol{u}_i}{dt} = m_i\,\boldsymbol{f}_i^C + m_i\,\boldsymbol{g}_i + \mathcal{Q}_i^V, \\ m_i\,I_i\dfrac{d\boldsymbol{\Omega}_i}{dt} = m_i\,\boldsymbol{t}_i^C + m_i\,\boldsymbol{G}_i + \mathcal{T}_i^V, \end{cases} \tag{15}$$

where $m_i\,\boldsymbol{f}_i^C$ is the interparticle conservative force, $\boldsymbol{g}_i$ the acceleration due to the conservative body forces, *i.e.* $\boldsymbol{g}_i = -\partial U/\partial \boldsymbol{r}_i$.The second equation of (15) governs the particle spin dynamics. In analogy with the first equation, the terms on the right-hand side are: $m_i\,\boldsymbol{t}_i^C$, the interparticle conservative torque, $\boldsymbol{G}_i$, the angular acceleration due to the body torque field linked to the potential $\mathcal{V}$, *i.e.* $\boldsymbol{G}_i = -\partial\mathcal{V}/\partial\boldsymbol{\theta}_i$.

Making use of the properties of internal energy e and translational invariance, one can write $m_i\,\boldsymbol{f}_i^c$ in equation 15 (see [5] for details) as:

$$\begin{aligned} m_i\,\boldsymbol{f}_i^C \equiv -\sum_j m_j\frac{\partial e_j}{\partial \boldsymbol{r}_i} &= -\sum_j m_j\frac{\partial e_j}{\partial \rho_j}\bigg|_s\frac{\partial \rho_j}{\partial \boldsymbol{r}_i} = \\ &= \sum_j\left[\frac{p_j\,V_j^2 + p_i\,V_i^2}{V_i\,V_j}\right]\boldsymbol{r}_{ij}F(r_{ij})\,V_i V_j, \end{aligned} \tag{16}$$

where we have used the fact that the particle pressure is linked to the internal energy: $p = \rho^2\,\partial e/\partial\rho\big|_s$. In this derivation we have considered that the entropy s is intrinsically carried by the particles and is not a function of the environment, as the local mass density ρ is. Considering that the density field is affected by the particle positions and not by the spatial rotations, in the present model $\boldsymbol{t}_i^C$ is assumed equal to zero.

Equations (15) are integrated in time to describe the dynamics of the system, including the formulated dissipative forces and torques.

B. Symmetries and conservation laws

The fact that the dissipative function has translational and rotational invariance guarantees that both the total momentum and the angular momentum is conserved in the particle-particle interaction, in analogy with the purely conservative systems. Following [20], one finds that the proposed dissipative interactions satisfy,

$$\begin{aligned} \sum_{i,j\neq i}\mathcal{Q}_{ij}^V &= \sum_{i,j<i}\mathcal{Q}_{ij}^V + \sum_{i,j>i}\mathcal{Q}_{ij}^V = \sum_{i,j<i}\mathcal{Q}_{ij}^V + \sum_{j,i<j}\mathcal{Q}_{ij}^V = \\ &= \sum_{i,j<i}\left(\mathcal{Q}_{ij}^V + \mathcal{Q}_{ji}^V\right) = 0 \end{aligned} \tag{17}$$

according to (14). Following the same procedure, the total dissipative torque exerted on the system satisfies,

$$\sum_{i,j\neq i}\left(\boldsymbol{r}_i\times\mathcal{Q}_{ij}^V + \mathcal{T}_{ij}^V\right) = \sum_{i,j<i}\left(\boldsymbol{r}_{ij}\times\mathcal{Q}_{ij}^V + 2\mathcal{T}_{ij}^V\right) = 0 \tag{18}$$

The null value of the total torque in the last equality is obtained by introducing eqs. (11) and (12) into (18). The proof that the same is valid for the conservative forces and torques can be found in the textbooks [11] and will be omitted here. Equations (17) and (18), together with the equivalent expressions for conservative forces and torques, make possible that the total system momentum $\sum_i m_i\frac{d\boldsymbol{u}_i}{dt} = 0$, as well as angular momentum $\sum_i(\boldsymbol{r}_i\times m_i\frac{d\boldsymbol{u}_i}{dt} + m_i\,I_i\frac{d\boldsymbol{\Omega}_i}{dt}) = 0$, which therefore are conserved.

Secondly, the total energy is not conserved due to the viscous forces and torques. However, we can verify that the

variation of the total entropy of the system is entirely given by the DF,

$$\sum_i \left[m_i T_i \frac{ds_i}{dt} \right] = - \sum_i \left[\mathcal{Q}_{ij}^V \cdot \boldsymbol{u}_i + \mathcal{T}_{ij}^V \cdot \boldsymbol{\Omega}_i \right] = \Phi_D \geq 0 . \quad (19)$$

Thus, the dissipative function must be positive-definite, which imposes conditions on the allowed values of the coefficients introduced in (9), namely,

$$\zeta_2 \geq 0 , \qquad \text{and} \qquad \zeta_1 \geq -\zeta_2 . \quad (20)$$

C. A general isotropic micropolar fluid model in SPH.

Inspired by Condiff & Dahler [6], the following dissipation function Φ'_D is now proposed, extending Φ_D defined in (7) to account for other possible dissipation mechanisms based on spin derivatives,

$$\Phi'_D = \Phi_D + \Phi_D^\Omega, \quad (21)$$

with

$$\Phi_D^\Omega = \sum_{i,j>i} \boldsymbol{\Omega}_{ij} \cdot \mathbb{B}_{ij}(r_{ij}) \cdot \boldsymbol{\Omega}_{ij} , \quad (22)$$

where $\boldsymbol{\Omega}_{ij} := \boldsymbol{\Omega}_i - \boldsymbol{\Omega}_j$, and where $\mathbb{B}$ is an objective tensor of second rank, with the same structure as $\mathbb{A}$ in (8):

$$\mathbb{B}_{ij}(r_{ij}) = F(r_{ij}) \left(\xi_1 \, \boldsymbol{e}_{ij} \otimes \boldsymbol{e}_{ij} + \xi_2 \, \boldsymbol{I} \right) V_i V_j . \quad (23)$$

This is the most general form that preserves translational and solid-body rotational invariance of the dissipation function in (22). It is noted that the dimensions of the viscosity coefficients ζ_1, ζ_2, and ξ_1, ξ_2 are different.
From eqs. (22) and (23), the following expression for Φ_D^Ω is obtained:

$$\begin{aligned} \Phi_D^\Omega = & \frac{\xi_1}{2} \sum_{i,j\neq i} F(r_{ij}) \, (\boldsymbol{e}_{ij} \cdot \boldsymbol{\Omega}_{ij})^2 \, V_i V_j \\ & + \frac{\xi_2}{2} \sum_{i,j\neq i} F(r_{ij}) \, \boldsymbol{\Omega}_{ij}^2 \, V_i V_j , \end{aligned} \quad (24)$$

Since Φ_D^Ω depends only on the spin derivatives, it impacts only on the viscous torque $m_i \, \boldsymbol{t}_i^v$, as computed with (15), redefined now as,

$$\begin{aligned} \mathcal{T}_i^V = & - \frac{\partial}{\partial \boldsymbol{\Omega}_i} \Phi_D - \frac{\partial}{\partial \boldsymbol{\Omega}_i} \Phi_D^\Omega = \\ = & \frac{\zeta_2}{2} \sum_j F(r_{ij}) \, \boldsymbol{r}_{ij} \times \left(\boldsymbol{u}_{ij} - \overline{\boldsymbol{\Omega}}_{ij} \times \boldsymbol{r}_{ij} \right) V_i V_j \\ & - \xi_1 \sum_j F(r_{ij}) \, (\boldsymbol{e}_{ij} \cdot \boldsymbol{\Omega}_{ij}) \, \boldsymbol{e}_{ij} \, V_i V_j \\ & - \xi_2 \sum_i F(r_{ij}) \, \boldsymbol{\Omega}_{ij} \, V_i V_j . \end{aligned} \quad (25)$$

This viscous torque completes the right hand side in (15) to yield the general micropolar model. The first term in (25) comes from Φ_D and was already presented in (12). The second and the third derive from Φ_D^Ω.

III. The continuum equations

The conservation laws derived from the dynamic equations of the SPH particles lead to a hydrodynamic motion of this ensemble according to a fluid with spin. The continuum limit is therefore important to identify the different viscosities in terms of the model parameters introduced, as well as to infer the scaling laws followed by the different model coefficients as a function of the characteristic length h. To derive these continuum equations, the time-derivative of the hydrodynamic fields, such as momentum, angular momentum and mass densities, constructed from the SPH particles, are expanded up to $O(h^2)$. The explicit derivation of the continuum equations is given in [20] and will be omitted here, although the final expressions are given.

The momentum transport equation for a fluid with spin reads,

$$\rho \frac{d\boldsymbol{u}}{dt} = - \nabla p + \rho \boldsymbol{f}^v + \rho \boldsymbol{g}. \quad (26)$$

with

$$\rho \boldsymbol{f}^v = (\mu + \mu_r) \, \nabla^2 \boldsymbol{u} + (\mu + \lambda - \mu_r) \nabla \, (\nabla \cdot \boldsymbol{u}) + 2\mu_r \nabla \times \boldsymbol{\Omega}, \quad (27)$$

where μ, λ and μ_r are the shear, second and microrotation viscosities, respectively. The comparison with the field equations of motion of the SPH model in the limit $h \to 0$ allows us to identify the relationship between the dissipative coefficients and the model parameters, which yield

$$\begin{cases} \mu = \dfrac{\zeta_1}{2(n+2)} + \dfrac{\zeta_2}{4}, \\ \lambda = \dfrac{\zeta_1}{2(n+2)}, \\ \mu_r = \dfrac{\zeta_2}{4} \qquad \Rightarrow \qquad \mu_r = \mu - \lambda. \end{cases} \quad (28)$$

According to (20), the following limits apply to μ, μ_r and λ:

$$\begin{cases} \mu \geq 0, \\ \mu_r \geq 0, \\ -\dfrac{2\mu}{n} \leq \lambda \leq \mu, \\ \qquad\qquad \Rightarrow \qquad 0 \leq \mu_r \leq \mu \left(1 + \frac{2}{n} \right). \end{cases} \quad (29)$$

The bulk viscosity κ_B, defined as (see [2]), reads,

$$\kappa_B = \lambda + \frac{2\mu}{n}, \quad (30)$$

The viscous force in (27) has the structure of the Newtonian one plus a rotational term. It is germane to mention that Müller et al. [17] proposed, for their model, this same dissipative term however with three degrees of freedom: a shear, a second and a rotational viscosity, postulating a-posteriori restrictions in their values. By deriving this force with a bottom-up approach from the particle level, it has been shown in the present article that

only two coefficients are actually independent if conservation laws must be satisfied.

The dynamic evolution of the field spin induced by (15) with (25) in the limit $h \to 0$ leads to the equation for the spin evolution at the continuous level:

$$\rho \mathcal{I} \frac{d\boldsymbol{\Omega}}{dt} = \rho \boldsymbol{G} - 2\mu_r (2\boldsymbol{\Omega} - \nabla \times \boldsymbol{u}) + + \gamma_1 \nabla^2 \boldsymbol{\Omega} + (\gamma_1 + \gamma_2) \nabla (\nabla \cdot \boldsymbol{\Omega}) \quad (31)$$

where the additional spin-viscosity coefficients γ_1 and γ_2 are linked to the parameters ξ_1 and ξ_2 through:

$$\gamma_1 = \left[\frac{\xi_1}{2(n+2)} + \frac{\xi_2}{2} \right], \qquad \gamma_2 = \left[\frac{\xi_1}{2(n+2)} - \frac{\xi_2}{2} \right], \quad (32)$$

and where we have implicitly assumed that $n \geq 3$. For $n = 2$, namely, in the case that two-dimensional simulations are performed (not to be confused with two dimensional flows studied through three-dimensional simulations), vorticity and spin are transported as scalars. Then, in (25) the term proportional to ξ_1 is exactly zero in $n = 2$ and should be ignored. In terms of viscosity coefficients, the latter implies that $\gamma_2 = -\gamma_1$. Hence, the transport coefficients given in (32), for two dimensions, correspond to the ones of (25) with $\xi_1 = 0$.

The evolution equation for the spin derivative (31) includes the same additional terms (spin Laplacian and gradient of spin divergence) like the corresponding one in the referred seminal paper by Condiff & Dahler [6] (equation 13 there).

The entropy production is now increased by Φ_D^Ω on the right-hand side of (19). Therefore, it follows that, in addition to (20), $\xi_2 \geq 0$ and $\xi_1 \geq -\xi_2$. It is worth noting that for planar flows $(\nabla \cdot \boldsymbol{\Omega})$ is zero.

It is important to notice that the moment of inertia in the continuum limit in the general case of a n-dimension fluid, scales as

$$I_i = c V_i^{2/n} + \mathcal{I} \quad (33)$$

where $\mathcal{I}$ is the moment of inertia of the molecular constituents of the fluid and c is a factor depending on the particle geometry (see [20] for a detailed discussion). For molecular fluids, the second term in this last equation is negligibly small. However, the first term is scale-dependent, as it is determined by the degree of coarse-grain (granularity) chosen for our simulation. Although no rotational inertia is present in the physical continuum fluid, still the simulation should consider a non-vanishing $I_i \sim h^2$ so that the total angular momentum is conserved in a SPH calculation with complex particle interactions. Furthermore, in the general model for fluids with spin, the micropolar effects can still be relevant even if the rotational inertia of the system is negligible in the continuum description. Effectively, when equating the left-hand side of (31) to zero, due to the presence of the new dissipative terms still the spin field $\boldsymbol{\Omega}$ is not equal to the vorticity but satisfies a spatial differential equation. It is thus expected that this general micropolar model can find application to the modelling of non-Newtonian fluids, in which the microscopic structure of the molecules can introduce this type of dissipative processes given in (24).

IV. Results

In ref. [20] we validate our new SPH model in two cases, namely, two-dimensional Poiseuille flow, for which it exist analytical solution, and the Lid-driven cavity, for which numerical solutions of the field equations via mesh methods are available. Excellent agreement was found in both cases. Here, we discuss only the second, for illustration purposes.

A. Lid-driven cavity with a micropolar fluid

The lid-driven cavity is a well-known benchmark case for validating numerical solvers on viscous flows. Its physical characteristics resemble those typical of lubrication processes, a field in which micropolar fluids have received great attention in the literature (see e.g. [1], [13], [22]). In 2012 Chen et al. [4] showed numerical simulations of a lid-driven cavity with a micropolar fluid, although they provided no velocity profiles. More recently, Venkatadri et al. [23] studied the same problem providing the 2D velocity profiles. These authors adopted the momentum (27) for modeling this problem, but using an equivalent but different definition of the viscosity parameters [9],

$$\rho \boldsymbol{f}^v = (\mu + \kappa) \nabla^2 \boldsymbol{u} + (\mu + \lambda) \nabla (\nabla \cdot \boldsymbol{u}) + \kappa \nabla \times \boldsymbol{\Omega}, \quad (34)$$

with the corresponding, also equivalent, spin equation:

$$\rho \mathcal{I} \frac{d\boldsymbol{\Omega}}{dt} = \rho \boldsymbol{G} - \kappa (2\boldsymbol{\Omega} - \nabla \times \boldsymbol{u}) \quad (35)$$

In this latter formulation the rotational viscosity is referred to as κ. When this alternative formulation is used, the dependence of its coefficients (μ, κ, λ) with ζ_1 and ζ_2 needs to be consistently readjusted, changing Eqs. (28) accordingly (see [20] for details). Venkatadri et al. studied the influence of selecting different values of $K = \kappa/\mu$ on the lid-driven cavity flow. Here, for the sake of brevity the cases $K = 0$ (that is standard Newtonian fluid) and $K = 3$ are treated with the proposed SPH model.

In the left panel of Fig. 2 the setup of the problem is shown along with the conditions on the walls. The Reynolds number is $\mathrm{Re} = \rho U L/\mu = 400$ and the spatial resolution is $N = L/\Delta r = 400$ where Δr is the initial particle distance. The right panel of the same figure displays the time history of the kinetic energy for $K = 0$ and $K = 3$. In this latter case, we observe a decrease of the kinetic energy at the steady state, as a consequence of an increase of dissipation due to the spin.

In Fig. 3 the streamlines for the two selected cases are shown. For $K = 3$, a positive vertical displacement of the central vortex is visible, as well as a mitigation of the recirculation vortex at the bottom right corner.

Finally, Fig. 4 shows the comparison between the mid-section velocity profiles as predicted by the present SPH model, by the finite difference schemes in Venkatadri et al. [23] and by the classic reference of Ghia et al [10] for the Newtonian case. As can be appreciated, the SPH simulation is in qualitative fair agreement with the reference results of the referred Eulerian schemes.

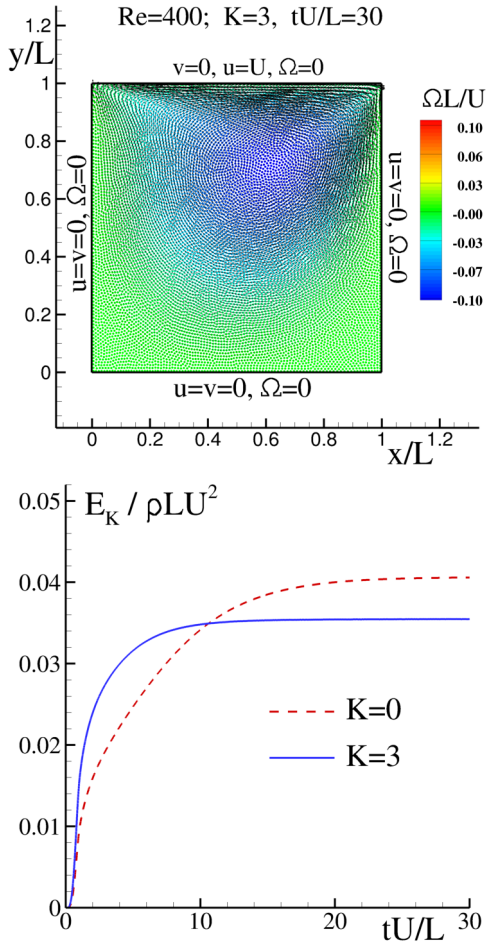

Fig. 2. Lid-driven cavity. Left: Sketch of the problem and of the boundary conditions. Right: time histories of the kinetic energy for $K = 0$ and $K = 3$. The spatial resolution is $N = L/\Delta r = 400$.

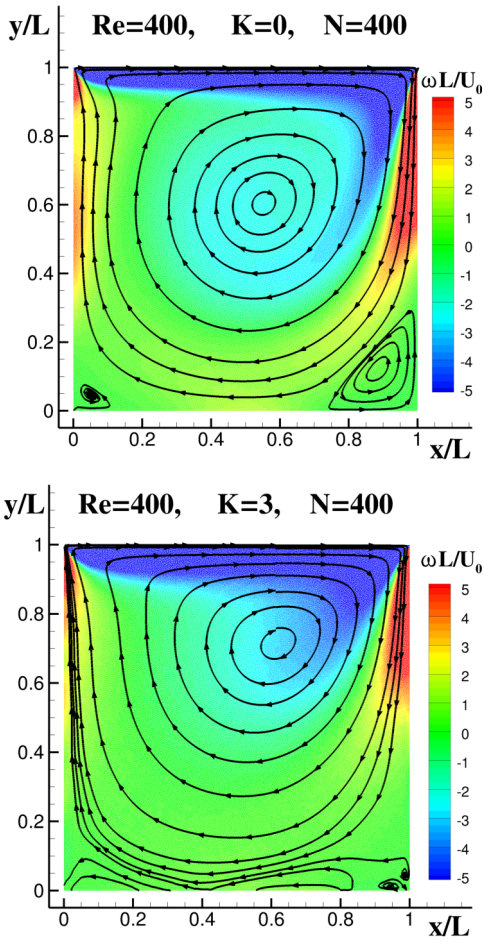

Fig. 3. Lid-driven steady-state streamlines for $Re = 400$, $\mu_r/\mu = 0$ (left), and $\mu_r/\mu = 2$ (right).

V. Conclusions

In this paper we have reviewed the previous bottom-up approaches [3], [5] to construct smoothed particle hydrodynamics (SPH) models from Lagrangian mechanics, supplemented with the addition of the Rayleighian or dissipation function (DF), as a powerful tool to enforce general principles of momenta conservation in complex systems. In the case of micropolar fluids analized here, a dissipation function has been defined at the particle level which depends on the relative velocity between particles but also on an additional spin degree of freedom, which modifies such relative velocity and introduces spin related intrinsic dissipation mechanisms, comparable to those related to the rate of deformation tensor in Newtonian fluids. This dissipation function is invariant under translations and solid-body rotations, which ensures that the resulting forces and torques will respect the conservation of the total momentum and angular momentum of the system. The dissipative forces derived from the dissipation function have been then incorporated to balance the expression obtained from the minimization of the Lagrangian of the system, leading to a set of SPH particle equations to describe the dynamics of the system in the most general case of micropolar fluid. The bottom-up approach has also allowed us to discuss in depth the nature of the moment of inertia per unit of mass of the SPH particles. The obtained discrete model has been taken to the continuum and compared with micropolar models from the literature, establishing the corresponding relationships between their coefficients and the ones of the dissipative terms considered at the particle level. The derivation of SPH equations from first principles, rather than from a discretization of the space, is thus a powerful tool to describe the behavior of complex systems or fluxes under extreme situations.

Acknowledgment

The research activity was partially developed within the Project Area Applied Mathematics of the Department of Engineering, ICT and Technology for Energy and Transport (DIITET) of the Italian National Research Council (CNR). J.B.A. wishes to thank the Cooperative Agreement no. W911NF-20-2-0027 of the US Army Research Office "Development of

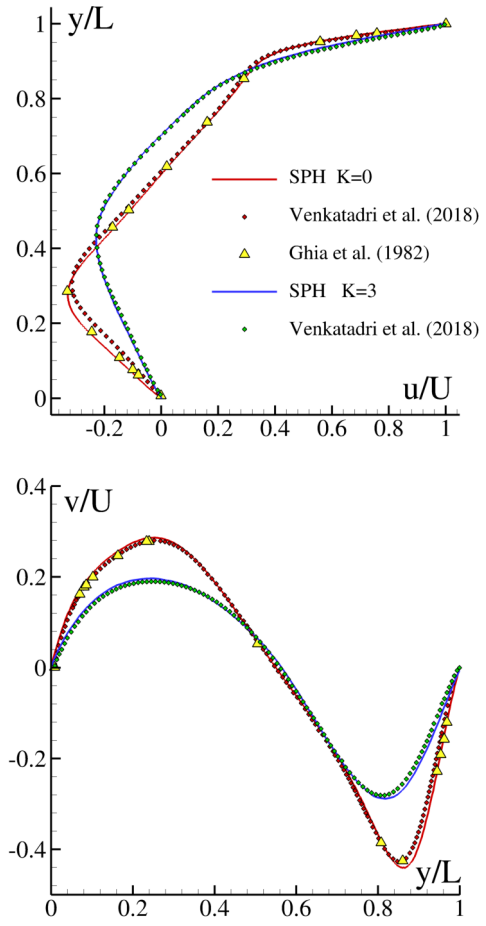

Fig. 4. Lid-driven cavity. Steady-state mid-section velocity profiles for $Re = 400$. Left: horizontal velocity component. Right: vertical velocity component.

Computational Capabilities to Simulate Energetic Materials at the Microscale". A.S.I. acknowledges the support of MCIU under grant RTI2018-096791-B-C21 "Hidrodinámica de elementos de amortiguamiento del movimiento de aerogeneradores flotantes".

References

[1] T. Ariman, M.A. Turk, and N.D. Sylvester. Applications of microcontinuum fluid mechanics. *International Journal of Engineering Science*, 12(4):273 – 293, 1974.

[2] R. Aris. *Vectors, Tensors, and the Basic Equations of Fluid Mechaniscs*. Dover Books on Mathematics Series. Dover Publications, Mineola, New York, 1989.

[3] Josep Bonet Avalos, Matteo Antuono, Andrea Colagrossi, and Antonio Souto-Iglesias. Shear-viscosity-independent bulk-viscosity term in smoothed particle hydrodynamics. *Phys. Rev. E*, 101:013302, Jan 2020.

[4] J Chen, C Liang, and J D Lee. Theory and simulation of micropolar fluid dynamics. *Proceedings of the Institution of Mechanical Engineers, Part N: Journal of Nanoengineering and Nanosystems*, 224(1-2):31–39, 2010.

[5] Andrea Colagrossi, Danilo Durante, Josep Bonet Avalos, and Antonio Souto-Iglesias. Discussion of Stokes' hypothesis through the smoothed particle hydrodynamics model. *Phys. Rev. E*, 96:023101, August 2017.

[6] Duane W. Condiff and John S. Dahler. Fluid mechanical aspects of antisymmetric stress. *The Physics of Fluids*, 7(6):842–854, 1964.

[7] R. Di Lisio, E. Grenier, and M. Pulvirenti. The convergence of the SPH method. *Computers and Mathematics with Applications*, 35(1–2):95–102, 1998.

[8] Masao Doi. Onsager's variational principle in soft matter. *J. Phys.: Condens. Matter*, 23(28):284118, jun 2011.

[9] A Cemal Eringen. Theory of micropolar fluids. *Journal of Mathematics and Mechanics*, pages 1–18, 1966.

[10] UKNG Ghia, Kirti N Ghia, and CT Shin. High-Re solutions for incompressible flow using the Navier-Stokes equations and a multigrid method. *Journal of computational physics*, 48(3):387–411, 1982.

[11] H Goldstein. *Classical Mechanics*. Addison-Wesley Publishing Company, 1996.

[12] J. P. Hansen and I. R. McDonald. *Theory of Simple Liquids*. Academic Press, London NW1 7DX, second edition, 1991.

[13] Pankaj Khatak and H. C. Garg. Performance Analysis of Capillary Compensated Hybrid Journal Bearing by Considering Combined Influence of Thermal Effects and Micropolar Lubricant. *Journal of Tribology*, 139(1), 08 2016. 011707.

[14] S. Mas-Gallic and P. A. Raviart. A particle method for first-order symmetric systems. *Numerische Mathematik*, 51:323–352, 1987. 10.1007/BF01400118.

[15] J. Monaghan and R. A. Gingold. Shock Simulation by the particle method SPH. *Journal of Computational Physics*, 52(2):374–389, 1983.

[16] Joseph P. Morris, Patrick J. Fox, and Yi Zhu. Modeling Low Reynolds Number Incompressible Flows Using SPH. *Journal of Computational Physics*, 136:214–226, 1997.

[17] Kathrin Muller, Dmitry A. Fedosov, and Gerhard Gompper. Smoothed dissipative particle dynamics with angular momentum conservation. *Journal of Computational Physics*, 281:301 – 315, 2015.

[18] Nathan J. Quinlan, Martin Lastiwka, and Mihai Basa. Truncation error in mesh-free particle methods. *International Journal for Numerical Methods in Engineering*, 66(13):2064–2085, 2006.

[19] A. Souto-Iglesias, J. Bonet Avalos, M. Antuono, and A. Colagrossi. General isotropic micropolar fluid model in smoothed particle hydrodynamics. *Physical Review E*, 104:015315, 7 2021.

[20] A. Souto-Iglesias, J. Bonet Avalos, M. Antuono, and A. Colagrossi. General isotropic micropolar fluid model in smoothed particle hydrodynamics. *Physical Review E*, 104:015315, 7 2021.

[21] V.K. Stokes. *Theories of Fluids with Microstructure: An Introduction*. Springer Berlin Heidelberg, 2012.

[22] Das Subrata and Guha Sisir Kumar. Non-linear stability analysis of micropolar fluid lubricated journal bearings with turbulent effect. 71(1):31–39, Jan 2019.

[23] K Venkatadri, S Maheswari, C Venkata Lakshmi, and V Ramachandra Prasad. Numerical simulation of lid-driven cavity flow of micropolar fluid. *IOP Conference Series: Materials Science and Engineering*, 402:012168, sep 2018.

[24] D. Violeau. Dissipative forces for Lagrangian models in computational fluid dynamics and application to smoothed-particle hydrodynamics. *Phys. Rev. E*, 80:036705, 2009.

[25] Damien Violeau and Thomas Fonty. Calculating the smoothing error in sph. *Computers & Fluids*, 191:104240, 2019.